

## COUPLING EFFECT FOR DIELECTRIC METAMATERIAL DIMER

F. Zhang<sup>1, \*</sup>, V. Sadaune<sup>2</sup>, L. Kang<sup>2</sup>, Q. Zhao<sup>3</sup>, J. Zhou<sup>4</sup>, and D. Lippens<sup>2</sup>

<sup>1</sup>Key Laboratory of Space Applied Physics and Chemistry, Ministry of Education and Department of Applied Physics, School of Science, Northwestern Polytechnical University, Xi'an 710072, P. R. China

<sup>2</sup>Institut d'Electronique de Microélectronique et de Nanotechnologie, CNRS 8520, Université des Sciences et technologies de Lille, 59652 Villeneuve d'Ascq Cedex, France

<sup>3</sup>State Key Lab of Tribology, Department of Precision Instruments and Mechanology, Tsinghua University, Beijing 100084, P. R. China

<sup>4</sup>State Key Lab of New Ceramics and Fine Processing, Department of Materials Science and Engineering, Tsinghua University, Beijing 100084, P. R. China

**Abstract**—In this paper, we report experimentally and numerically on coupling effects of dielectric metamaterial dimer (metadimer) which composed of two identical ceramic cubes with high permittivity. The distance dependence of Mie resonance for metadimer is investigated under various polarizations of external wave. By changing the configurations and alignment of dimer resonator, it is revealed that magnetic and electric resonances of metadimer exhibits a red/blue shift, resulting from longitudinal or transverse coupling effects of dipoles. Besides, quasi bound states between tightly stacked dielectric cubes are also been pointed out for electric Mie resonance, which is responsible for an unexpected frequency shift with a reverse variation.

### 1. INTRODUCTION

Electromagnetic metamaterials with exotic properties have attracted increasing attention during past decade [1]. Various novel devices based on metamaterial including perfect absorber [2–6]

---

*Received 13 August 2012, Accepted 27 September 2012, Scheduled 16 October 2012*

\* Corresponding author: Fuli Zhang (fuli.zhang@nwpu.edu.cn).

have been developed. Up to now, most of present metamaterial configuration are constructed by using artificial microstructures such as split ring resonator (SRR) or wire [7–13], whose size and periodicity are far smaller than the operating wavelengths so that the response of metamaterial to electromagnetic/optics wave can be interpreted by using effective parameters [14–16]. Generally, the macroscopic behaviours of metamaterial structure derived from effective electromagnetic parameters are engineered by the basic microstructure element, i.e., metamolecule. Following effective medium theory, various metamaterial related devices can be designed by using simplified model, from which only average response of individual element is considered whereas coupling effect between individual elements has been ignored in most cases. However, in analogy to the interplaying effect of atoms which is of greatly importance on the determination of optical spectroscopy behaviours of common materials, the interaction between neighbouring metamaterial elements always exists and plays an important role to the determination of the resonance frequency location as well as the emergence of novel resonance mode [17–23].

So far, most works were concentrated on the coupling effects of SRRs, providing more means to control electromagnetic/optics wave. On the other hand, artificial magnetism can be also produced via Mie resonance of dielectric particles with relative high permittivity [24–43]. From Mie theory [24–26], it can be analytically demonstrated that the electromagnetic wave interaction of dielectric particles may exhibit a strong magnetic or electric resonances. From the oscillation of resulting magnetic/electric dipole, negative permeability/permittivity may be produced. Compared to conventional planar SRR and related structures, Mie resonance metamaterial does not suffer from conductive currents and capacitance gap, so that it can be expected to generate low loss isotropic metamaterial structure [35–41]. This advantage is more remarkable at THz and optical regime owing to the limitation of high inductive loss and kinetic inductance of electrons [38–40]. However, the coupling effect of Mie resonance type metamaterial remains largely unexplored until now. For instance, Lai et al. reported a negative index behavior by using the single zirconia resonator with a combination of displacement current and Mie resonance [41]. Wheeler et al. investigated on the coupling effect by restricting their analysis to the interaction on the magnetic dipole of dielectric particle clusters [42]. We have recently reported numerical analysis of the periodicity variation influences on resonance state of arrayed dielectric particles [43].

As a two-cell system offers most elementary test-bed for study

of the fundamental interaction between individual units [44,45], we propose here a numerical and experimental study of dielectric metamaterial dimer (metadimer) which consists of two identical ceramic resonators. Unlike previous coupling effect investigations were mostly carried out inside element array, a single dielectric metadimer gives an insight of pure interplaying forces between its individual constituents. Electromagnetic response of such a dielectric dimer is investigated by changing the spacing between constituent resonators under different orientations of electromagnetic fields. Experiment and simulation results reveal that magnetic and electric resonance of dielectric metadimer can be dynamically tuned with red/blue frequency shift, arising from the longitudinal/transverse coupling effects of induced magnetic/electric dipoles. Furthermore, the emergence of bounding resonant state for close-packed metadimer is responsible for an abnormal frequency shift of electric resonance.

The manuscript is organized as follows, In Section 2, we will show the electromagnetic response of an individual dielectric resonator. The distance dependence of magnetic and electric resonances for dielectric metadimer and underlying physics interpretation are given in Section 3. The conclusion and remarks are outlined in Section 4.

## 2. ELEMENTARY CELL FOR DIELECTRIC METADIMER

At the first stage for the investigation of coupling effect of dielectric metadimer, we check the electromagnetic response of metadimer constituent, i.e., individual dielectric cubes. Such dielectric cubes

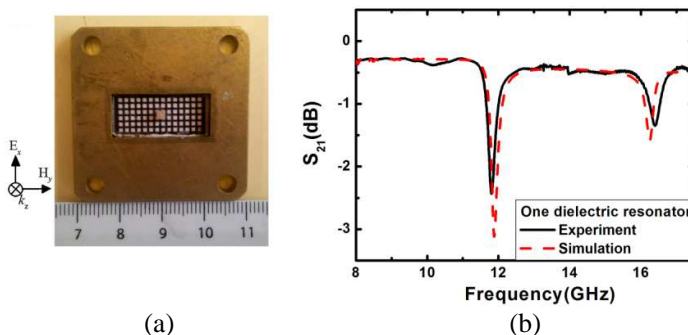


**Figure 1.** (a) Close up view and (b) transmission spectra for single dielectric metamaterial resonator located on a Teflon template inside a rectangular waveguide. Two type of rectangular waveguides were used for X and Ku band measurements, respectively.

were synthesized by using Barium Strontium Titanate (BST) ceramic with a relative high permittivity and modest dielectric loss ( $\epsilon_r = 132$ ,  $\tan \delta = 0.015$ ). The dielectric cubic resonator has a side length of 1.8 mm. The intrinsic high symmetry shape of dielectric resonator enables us to design, fabricate isotropic metamaterial. As shown in Figure 1(a), single dielectric resonator was stuck on a thin epoxy film whose surface was printed by square grid array to assist the determination of sample location. A Teflon substrate ( $\epsilon_r = 2.1$ ,  $\tan \delta = 0.001$ ) was used to support sample.

The transmission response of single dielectric resonator was measured using hollow waveguide system. To observe various Mie resonances, two types of standard rectangular waveguides, WR 90 and WR 60, were employed to cover microwave regime from 8.0 GHz to 18.0 GHz, respectively. The dielectric resonator is illuminated by an incident wave with electric polarization along the  $x$  axis and magnetic polarized along the  $y$  axis. From the transmission spectra shown in Figure 1(b), we can see that single dielectric resonator exhibits two vanishing transmission dips at 11.8 GHz and 16.5 GHz, corresponding to the first and second order Mie resonances, respectively. Numerical prediction of the transmission spectra were calculated by using commercial time domain package, CST microwave studio TM with reference. A good fit between experiment and simulation can be observed. A slight variation on the resonance frequency position and strength is presumably due to minor fabrication tolerance.

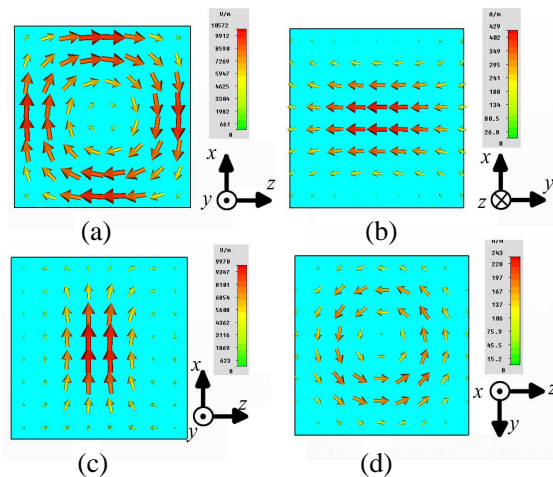


**Figure 2.** (a) (c) Local electric and (b) (d) magnetic field inside single dielectric metamaterial resonator for the first and second Mie resonances occurring at 11.8 GHz and 16.5 GHz, respectively.

To clarify the underlying physics for these two resonances, local field was monitored and displayed in Figure 2. Around the first Mie resonance, induced circulation of displacement currents leads to a nonzero magnetic dipole momentum opposite to that of incident magnetic field, therefore, demonstrating a magnetic resonance characteristic. On the other hand, local electric field oscillates along the  $x$  axis, thereby corresponding to an electric resonance around the second Mie resonance. At the vicinities of various Mie resonances of dielectric resonator, the resulting magnetic/electric dipole momentum provides the possibility to achieve effective electromagnetic parameters below unity or even zero [35–41].

### 3. DIELECTRIC DIMER

In the following section, we will focus on the electromagnetic response of dielectric metadimer by varying BST cube separation and its orientation with respect to incident wave. As shown in Figure 3, considering metadimer axis orientation, we investigate metadimer with its axis parallel and perpendicular to external electric field. For the case of metadimer axis perpendicular to incident electric polarization, the dimer with its axis parallel to the magnetic field and wave vector  $k$  are studied. For each configuration of metadimer, the separation between dielectric resonators was varied gradually to give a detailed

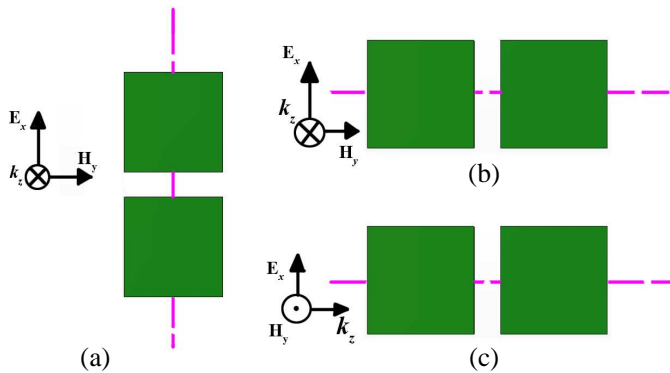


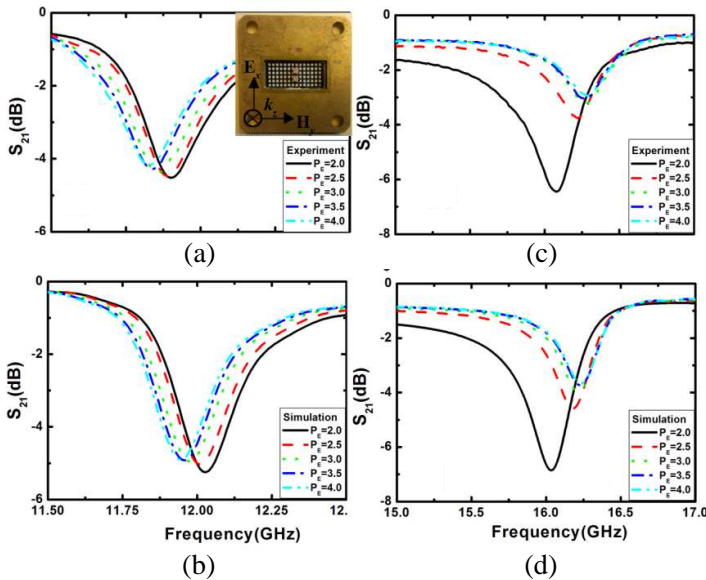
**Figure 3.** Schematic view of dielectric metadimer under various excitation of external electromagnetic wave. (a) Incident electric field is parallel to the metadimer axis (purple dashed line). For the electric field perpendicular to the metadimer axis, two resonators are stacked (b) perpendicular and (c) parallel to the incident wave propagation direction.

observation for the influences on magnetic and electric Mie resonances. For the sake of simplicity, we refer metadimer separation along  $\mathbf{E}$ ,  $\mathbf{H}$ , and  $\mathbf{k}$  directions to as  $P_E$ ,  $P_H$  and  $P_k$ .

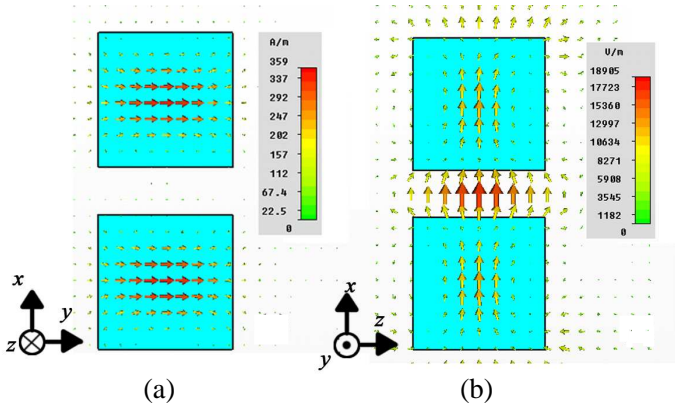
### 3.1. Dielectric Metadimer Axis Parallel to Electric Field

Figure 4 shows the transmission spectra for dielectric metadimer with varying  $P_E$ . For individual resonator arranged by a separation of  $P_E = 4.0$  mm, metadimer shows two extinction dips located around 11.83 GHz and 16.28 GHz, corresponding to magnetic and electric Mie resonances, respectively. In comparison with individual resonator behavior, the nearly unchanged resonance frequencies imply the coupling effect between individual resonators is rather weak for relatively large separation. Besides, enhanced dip strength can be noted due to the increase of filling density.

As the dimer separation,  $P_E$ , decreases gradually from 4.0 mm down to 2.0 mm, magnetic resonance,  $f_{MR}$ , increases slightly from 11.83 GHz up to 11.90 GHz, whereas electric resonance,  $f_{ER}$ , shifts gradually from 16.29 GHz down to 16.08 GHz. This opposite distance



**Figure 4.** (a) (c) Experimental and (b) (d) simulated transmission spectra for the first and second Mie resonance of metadimer. The inset shows dielectric resonators stacked along the  $\mathbf{E}$  field and illuminated inside waveguide.



**Figure 5.** Local (a) magnetic and (b) electric field for dielectric dimer ( $P_E = 2.5$  mm) at magnetic and electric Mie resonances, respectively.

dependences of metadimer’s magnetic and electric resonances are also reproduced by full wave electromagnetic simulations.

To investigate the underlying physics of contrary frequency trend, we plot local field for metadimer with a separation of  $P_E = 2.5$  mm in Figure 5. From local field monitored around the corresponding Mie resonance frequencies, it can be seen that, magnetic field from each resonator are localized parallel to each other, forming transverse induced magnetic dipoles whose interaction forces are dominated by repulsive force. As a consequence, tighter configuration of metadimer leads to enhanced transverse magnetic coupling effect, thereby higher magnetic resonance frequency. On the contrary, for the second Mie resonance, neighbouring electric dipoles are polarized in an “end-to-end” state, i.e., positive ends of electric dipole are attracted by the negative one of neighboring electric dipole, giving rise to longitudinal coupling effects, which directly lowers the resonance frequency with decreasing  $P_E$  [23–27].

### 3.2. Dielectric Metadimer Axis Perpendicular to Electric Field

#### 3.2.1. Metadimer Separation Varies along $\mathbf{H}$ Field Direction

In this section, metadimer was formed with its axis along the  $\mathbf{H}$  field direction. Figure 6 shows the distance dependent transmission spectra for metadimer. As dielectric resonators are placed close to each other, the magnetic resonance of metadimer,  $f_{MR}$ , moves gradually from 11.67 GHz down to 11.07 GHz, accounting for frequency shift of 600 MHz with respect to the variation of  $\mathbf{P}_H$  by 2.0 mm. Furthermore,

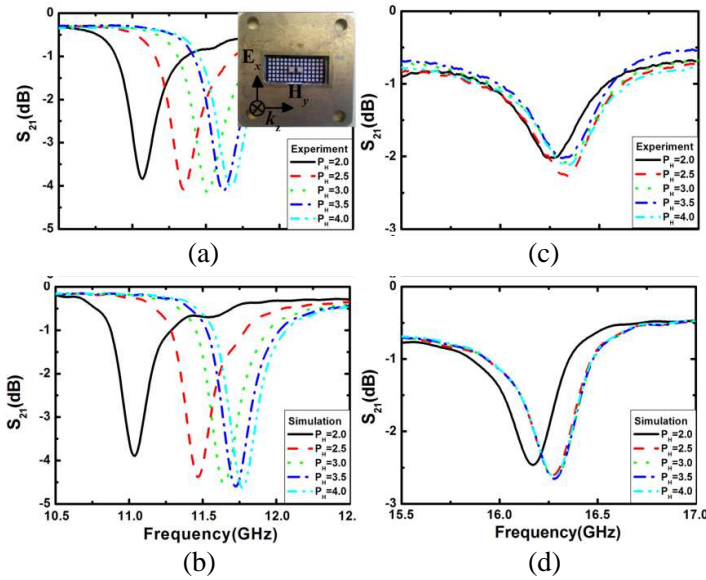


**Figure 6.** (a) (c) Experimental and (b) (d) simulated transmission spectra for the first and second Mie resonance of metadimer with its axis along the  $\mathbf{H}$  direction, respectively. The inset shows the dielectric metadimer is placed along the  $\mathbf{H}$  field inside a standard waveguide.

the magnetic resonance of metadimer shift becomes more visible since the  $\mathbf{P}_H$  decreases below 3.0 mm, demonstrating nonlinear frequency dependence with dimer separation along the  $\mathbf{H}$  field.

Figure 7(a) depicts local magnetic field for metadimer with its axis along the  $\mathbf{H}$  field directions at first Mie resonance frequency. From the local magnetic field distribution between neighbouring dielectric resonators, it can be demonstrated that the lower frequency shift for magnetic Mie resonance results from longitudinal magnetic field distribution inside metadimer.

For the electric resonance located around 16.0 GHz, metadimer shows a nearly independent property on the spacing variation until  $\mathbf{P}_H$  decreases below 2.5 mm, indicative of weak coupling effect of electric resonance. This frequency tendency of metadimer on  $\mathbf{P}_H$  is also verified by rigorous numerical calculation. Moreover, electric resonance frequency,  $f_{ER}$ , is shifted from 16.35 GHz down to 16.25 GHz as spacing distance is further decreased to 2.0 mm. However, this result is on the contrary to the anticipation of a higher frequency shift of,  $f_{ER}$ , with respect to smaller distance along  $\mathbf{H}$  direction, because of the transverse electric dipole configuration (Figure 7(b)). In order to clarify the underlying mechanism, we bring the comparison of local electric

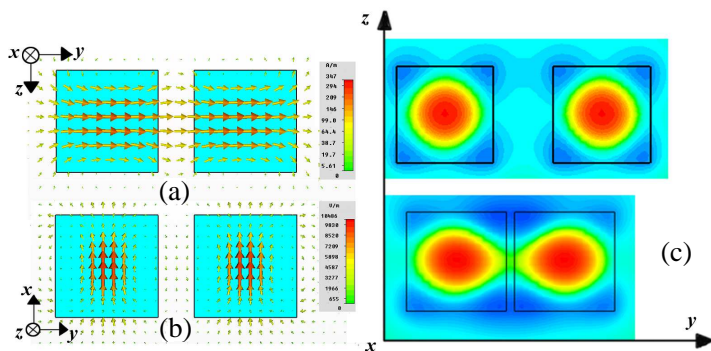


**Figure 7.** Local (a) magnetic and (b) electric field of meta-dimer ( $P_H = 2.5$  mm) around the first and second Mie resonance frequencies, respectively. (c) Local electric field component  $E_x$  of meta-dimer with separation of  $P_H = 3.0$  mm (Top panel) and  $P_H = 2.0$  mm (Bottom panel) around electric Mie resonance.

field for metadimer with different spacing. As seen in Figure 7(c), for dielectric metadimer with relative large spacing, the induced electric field is localized in the center of each dielectric resonator. As the two resonators approaches to each other, local electric field distribution changes gradually to form a quasi-bounding resonance mode for the dimer with  $P_H = 2.0$  mm, which is responsible for electric resonance frequency decrease. We also checked distance dependence of electric frequency for metadimer formed by two dielectric spheres. The emergence of quasi-bounding is more significant for close-placed dielectric spheres (Not shown here).

### 3.2.2. Metadimer Separation Varies along $k$ Direction

In this part, we placed Teflon substrate parallel to the incident wave propagation direction, so that we can investigate electromagnetic response of metadimer by varying interspacing along the  $k$  direction. The separation dependence of metadimer with its axis along the  $k$  direction is presented in Figure 8. As two resonators approach to each other, original magnetic resonance frequency,  $f_{MR}$ , moves slightly to higher frequency. Meanwhile, an extra minor dip emerges at low frequency, and becomes more evident. In addition, this feature exhibits a red-shift for the decreasing  $P_k$ , showing a completely different frequency dependence on the interspacing in comparison with that of original magnetic resonance. The local magnetic field component,  $H_y$ , as shown in Figure 9(a), clearly show that lower frequency dip

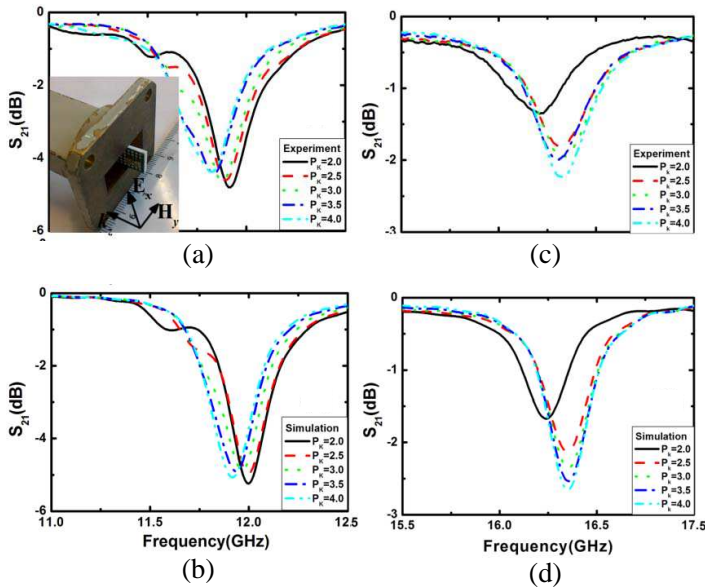


**Figure 8.** (a) (c) Experimental and (b) (d) simulated transmission spectra for the first and second Mie resonance of metadimer with its axis along  $k$  direction, respectively. The inset shows the dielectric metadimer is placed along  $k$  direction inside a standard waveguide.

is caused by the anti-phase oscillation of magnetic field between two resonators, leaving an attractive force inside metadimer, and lowering magnetic resonance frequency. On the contrary, an in-phase excitation of magnetic field forming a transverse coupling effect explains the reason why the main magnetic resonance dip increases with higher density of metadimer.

The electric Mie resonance of metadimer as a function of various spacing of  $P_k$  is also studied and presented in Figure 8. Unlike magnetic resonance frequency dependence, only single electric resonance dip occurs around 16.3 GHz during the interspacing variation. This does not mean only one electric resonant state of dimer excited, since we observed numerically in-/anti-phase electric oscillation for neighbouring resonators with a relatively smaller dielectric loss (Not shown here). Moreover, the electric resonance frequency,  $f_{ER}$ , exhibits almost independence of interspacing change except for a low frequency shift for  $P_k = 2.0$  mm. This variation is very similar to that of metadimer with small separation along the  $\mathbf{H}$  direction, as electric field polarizations are the same in both cases. This anticipation is further confirmed by the local electric field, which demonstrates that a quasi-bounding

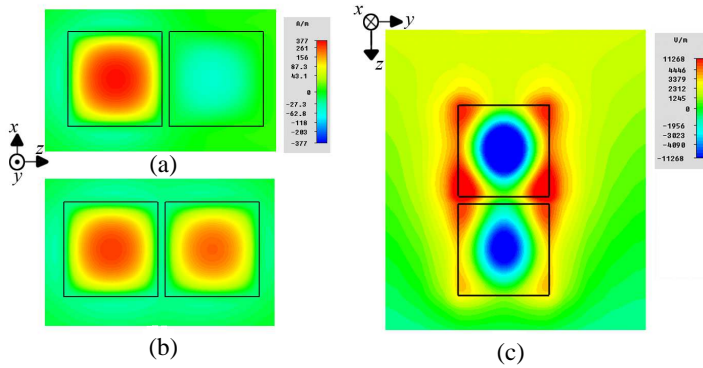


**Figure 9.** Local magnetic field component  $H_y$  at (a) lower and (b) higher magnetic resonance frequencies for metadimer with its axis along propagation direction. (c) Local electric field component  $E_x$  around electric resonance frequency ( $P_k = 2.0$  mm).

mode occurs between close dielectric resonators stacked along the wave vector direction (See Figure 9(c)).

#### 4. CONCLUSION

In this manuscript, we presented the coupling effect inside dielectric metamaterial dimer. By varying the interspacing of metadimer along various configurations with respect to the incident wave, it is verified that both magnetic and electric Mie resonances of dielectric metamaterial dimer can be tailored red/blue shift via different configurations of constitutive resonators. It is well interpreted with transverse/longitudinal coupling effect of magnetic/electric dipole. Moreover, new emergence resonance mode for electric Mie resonance is responsible for the unexpected frequency shift for metadimer. In comparison with the individual dielectric resonator, the separation dependence of metadimer response offers more way to tailor the magnetic and electric resonances. Since Mie resonance of particles is quite general from microwave to optical range [37, 38], we believe that underlying physics mechanism for metadimer, revealed in this manuscript, will be helpful to provide more degrees of freedom to design and control new structure of artificial electromagnetic structure in high frequency regime.

#### ACKNOWLEDGMENT

We gratefully acknowledge the financial support from the National Natural Science Foundation of China (Grant Nos. 61101044, 61275176,

60978053, 90922025, 51032003, 50921061), National High Technology Research and Development Program of China (863 Program) (Grant No. 2012AA030403), Project-sponsored by SRF for ROCS, SEM, NPU Foundation for Fundamental Research (Grant No. NPU-FFR-JC20100243), NPU Aoxiang Star Project, and Research Fund for the Doctoral Program of Higher Education of China (Grant No. 20090002120008).

## REFERENCES

1. Shelby, R. A., D. R. Smith, and S. Schultz, "Experimental verification of a negative index of refraction," *Science*, Vol. 292, 77–79, 2001.
2. Landy, N. I., S. Sajuyigbe, J. J. Mock, D. R. Smith, and W. J. Padilla, "Perfect metamaterial absorber," *Phys. Rev. Lett.*, Vol. 100, 207402, 2008.
3. Zhu, B., Z. Wang, C. Huang, Y. Feng, J. Zhao, and T. Jiang, "Polarization insensitive metamaterial absorber with wide incident angle," *Progress In Electromagnetics Research*, Vol. 101, 231–239, 2010.
4. Li, M., H.-L. Yang, X.-W. Hou, Y. Tian, and D.-Y. Hou, "Perfect metamaterial absorber with dual bands," *Progress In Electromagnetics Research*, Vol. 108, 37–49, 2010.
5. Huang, L. and H. Chen, "Multi-band and polarization insensitive metamaterial absorber," *Progress In Electromagnetics Research*, Vol. 113, 103–110, 2011.
6. He, X.-J., Y. Wang, J. Wang, T. Gui, and Q. Wu, "Dual-band terahertz metamaterial absorber with polarization insensitivity and wide incident angle," *Progress In Electromagnetics Research*, Vol. 115, 381–397, 2011.
7. Pendry, J. B., A. J. Holden, D. J. Robbins, and W. J. Stewart, "Magnetism from conductors and enhanced nonlinear phenomena," *IEEE Trans. Microw. Theory Tech.*, Vol. 47, 2075–2084, 1999.
8. Pendry, J. B., A. J. Holden, W. J. Stewart, and I. Youngs, "Extremely low frequency plasmons in metallic mesostructures," *Phys. Rev. Lett.*, Vol. 76, 4773–4776, 1996.
9. Marqués, R., F. Mesa, J. Martel, and F. Medina, "Comparative analysis of edge and broadside coupled split ring resonators for metamaterial design — Theory and experiments," *IEEE Trans. Antennas Propag.*, Vol. 51, 2572–2581, 2003.
10. Chen, H., L.-X. Ran, J. T. Huang-Fu, X.-M. Zhang, K.-S. Cheng,

- T. M. Grzegorzcyk, and J. A. Kong, "Magnetic properties of S-shaped split-ring resonators," *Progress In Electromagnetics Research*, Vol. 51, 231–247, 2005.
11. Chen, H., L. Ran, J. Huangfu, X. Zhang, K. Chen, T. M. Grzegorzcyk, and J. A. Kong, "Left-handed materials composed of only S-shaped resonators," *Phys. Rev. E*, Vol. 70, 057605, 2004.
  12. Feng, T., Y. Li, H. Jiang, W. Li, F. Yang, X. Dong, and H. Chen, "Tunable single-negative metamaterials based on microstrip transmission line with varactor diodes loading," *Progress In Electromagnetics Research*, Vol. 120, 35–50, 2011.
  13. Ourir, A., R. Abdeddaim, and J. de Rosny, "Tunable trapped mode in symmetric resonator designed for metamaterials," *Progress In Electromagnetics Research*, Vol. 101, 115–123, 2010.
  14. Smith, D. R., S. Schultz, P. Markoš, and C. M. Soukoulis, "Determination of effective permittivity and permeability of metamaterials from reflection and transmission coefficients," *Phys. Rev. B*, Vol. 65, 195104, 2002.
  15. Chen, X., T. M. Grzegorzcyk, B.-I. Wu, J. Pacheco, and J. A. Kong, "Robust method to retrieve the constitutive effective parameters of metamaterials," *Phys. Rev. E*, Vol. 70, 016608, 2004.
  16. Croënne, C., B. Fabre, D. Gaillot, O. Vanbésien, and D. Lippens, "Bloch impedance in negative index photonic crystals," *Phys. Rev. B*, Vol. 77, 125333, 2008.
  17. Liu, H., J. X. Cao, S. N. Zhu, N. Liu, R. Ameling, and H. Giessen, "Lagrange model for the chiral optical properties of stereometamaterials," *Phys. Rev. B*, Vol. 81, 241403(R), 2010.
  18. Liu, H., Y. M. Liu, T. Li, S. M. Wang, S. N. Zhu, and X. Zhang, "Coupled magnetic plasmons in metamaterials," *Phys. Status Solidi B*, Vol. 246, 1397, 2009.
  19. Liu, N. and H. Giessen, "Coupling effects in optical metamaterials," *Angew. Chem. Int. Ed.*, Vol. 49, 9838–9852, 2010.
  20. Feth, N., M. König, M. Husnik, K. Stannigel, J. Niegemann, K. Busch, M. Wegener, and S. Linden, "Electromagnetic interaction of split-ring resonators: The role of separation and relative orientation," *Opt. Express*, Vol. 18, 6545–6554, 2010.
  21. Sersic, I., M. Frimmer, E. Verhagen, and A. F. Koenderink, "Electric and magnetic dipole coupling in near-infrared split-ring metamaterial arrays," *Phys. Rev. Lett.*, Vol. 103, 213902, 2010.
  22. Carbonell, J., E. Lheurette, and D. Lippens, "From rejection to transmission with stacked arrays of split ring resonators," *Progress*

- In Electromagnetics Research*, Vol. 112, 215–224, 2011.
23. Zhang, F., Q. Zhao, J. Sun, J. Zhou, and D. Lippens, “Coupling effect of split ring resonator and its mirror image,” *Progress In Electromagnetics Research*, Vol. 124, 233–247, 2012.
  24. Lewin, L., “The electrical constants of a material loaded with spherical particles,” *Proc. Inst. Electr. Eng.*, Vol. 94, 65–68, 1947.
  25. Bohren, C. F. and D. R. Huffman, *Absorption and Scattering of Light by Small Particles*, Wiley, New York, 1998.
  26. O’Brien, S. and J. B. Pendry, “Photonic band-gap effects and magnetic activity in dielectric composites,” *J. Phys. Condens. Matt.*, Vol. 14, 4035–4044, 2002.
  27. Holloway, C. H., E. F. Kuester, J. Baker-Jarvis, and P. Kabos, “A double negative (dng) composite medium composed of magnetodielectric spherical particles embedded in a matrix,” *IEEE Trans. Antennas Propag.*, Vol. 51, 2596–2603, 2003.
  28. Zhao, Q., J. Zhou, F. Zhang, and D. Lippens, “Mie resonance-based dielectric metamaterial,” *Mater. Today*, Vol. 12, 36–45, 2009.
  29. Liu, L., J. Sun, X. Fu, J. Zhou, Q. Zhao, B. Fu, J. Liao, and D. Lippens, “Artificial magnetic properties of dielectric metamaterials in terms of effective circuit model,” *Progress In Electromagnetics Research*, Vol. 116, 159–170, 2011.
  30. Kang, L., V. Sadaune, and D. Lippens, “Numerical analysis of enhanced transmission through a single subwavelength aperture based on mie resonance single particle,” *Progress In Electromagnetics Research*, Vol. 113, 211–226, 2011.
  31. Lepetit, T., É. Akmansoy, and J.-P. Ganne, “Experimental measurement of negative index in an all-dielectric metamaterial,” *Appl. Phys. Lett.*, Vol. 95, 121101, 2009.
  32. Lin, X. Q., T. J. Cui, J. Y. Chin, X. M. Yang, Q. Cheng, and R. Liu, “Controlling electromagnetic waves using tunable gradient dielectric metamaterial lens,” *Appl. Phys. Lett.*, Vol. 92, 131904, 2008.
  33. Kozlov, D. S., M. A. Odit, I. B. Vendik, Y.-G. Roh, S. Cheon, and C.-W. Lee, “Tunable terahertz metamaterial based on resonant dielectric inclusions with disturbed Mie resonance,” *Appl. Phys. A*, Vol. 106, 465–470, 2012.
  34. Peng, L., L. Ran, H. Chen, H. Zhang, J. A. Kong, and T. M. Grzegorzcyk, “Experimental observation of left-handed behavior in an array of standard dielectric resonators,” *Phys. Rev. Lett.*, Vol. 98, 157403, 2007.

35. Zhao, Q., L. Kang, B. Du, H. Zhao, Q. Xie, X. Huang, B. Li, J. Zhou, and L. Li, "Experimental demonstration of isotropic negative permeability in a three-dimensional dielectric composite," *Phys. Rev. Lett.*, Vol. 101, 027402, 2008.
36. Zhang, F., Q. Zhao, L. Kang, J. Zhou, and D. Lippens, "Experimental verification of isotropic and polarization properties of high permittivity-based metamaterial," *Phys. Rev. B*, Vol. 80, 195119, 2009.
37. Schuller, J. A., R. Zia, T. Taubner, and M. L. Brongersma, "Dielectric metamaterials based on electric and magnetic resonances of silicon carbide particles," *Phys. Rev. Lett.*, Vol. 99, 107401, 2007.
38. Popa, B.-I. and S. A. Cummer, "Full-wave simulations of electromagnetic cloaking structures," *Phys. Rev. Lett.*, Vol. 100, 207401, 2008.
39. Ginn, J. C., I. Brene, D. W. Peters, J. R. Wendt, J. O. Stevens, P. F. Hines, L. I. Basilio, L. K. Warne, J. F. Ihlefeld, P. G. Clem, and M. B. Sinclair, "Realizing optical magnetism from dielectric metamaterials," *Phys. Rev. Lett.*, Vol. 108, 097402, 2012.
40. Miroshnichenko, A. E., B. Luk'yanchuk, S. A. Maier, and Y. S. Kivshar, "Optically induced interaction of magnetic moments in hybrid metamaterials," *Acs Nano*, Vol. 6, 837–842, 2012.
41. Lai, Y. J., C. K. Chen, and T. J. Yen, "Creating negative refractive identity via single dielectric resonators," *Opt. Express*, Vol. 17, 12960–12970, 2009.
42. Wheeler, M. S., J. S. Aitchison, and M. Mojahedi, "Coupled magnetic dipole resonances in sub-wavelength dielectric particle clusters," *J. Opt. Soc. Am. B*, Vol. 27, 1083–1091, 2010.
43. Zhang, F., L. Kang, Q. Zhao, J. Zhou, and D. Lippens, "Magnetic and electric coupling effects of dielectric metamaterial," *New J. Phys.*, Vol. 14, 033031, 2012.
44. Cao, L., P. Fan, and M. L. Brongersma, "Optical coupling of deep-subwavelength semiconductor nanowires," *Nano Lett.*, Vol. 11, 1461–1468, 2010.
45. Hao, E. and G. C. Schatz, "Electromagnetic fields around silver nanoparticles and dimmers," *J. Chem. Phys.*, Vol. 120, 357–366, 2004.